Macromolecules
ARTICLE

Macromolecules **2010**, *43*, 805–810 **805**
DOI: 10.1021/ma9021828

Thermotropic Liquid Crystalline Polyimides with Siloxane Linkages: Synthesis, Characterization, and Liquid Crystalline Behavior

Yu Shoji, Ryohei Ishige, Tomoya Higashihara, Junji Watanabe, and Mitsuru Ueda*

Department of Organic and Polymeric Materials, Graduate School of Science and Engineering, Tokyo Institute of Technology, 2-12-1-H-120, O-okayama, Meguro-Ku, Tokyo 152-8552, Japan

Received October 2, 2009; Revised Manuscript Received November 4, 2009

ABSTRACT: Thermotropic liquid crystalline (LC) semialiphatic polyimides have been developed from diamines containing siloxane spacer units with pyromellitic dianhydride (PMDA) or 3,3′,4,4′-tetracarboxybiphenyl dianhydride (BPDA). Monomer diamines with siloxane units were prepared by three steps, which include Williamson's synthesis, hydrosilylation, and reduction. The polymerization was conducted by the conventional method, solution polymerization, followed by thermal imidization. A highly viscose poly(amic acid) solution was obtained and its inherent viscosities were 0.65−1.73 dL/g. These novel polyimides exhibited high thermal stability and a lower crystal-LC transition temperature compared to reported polyimides containing alkylene or oxyethylene spacer units. X-ray studies were performed for investigating the oriented smectic mesophases of each polyimide. In the polyimides derived from PMDA, a smectic A (SmA) phase was formed on gradual cooling from the isotropic liquid phase. On the other hand, the polyimides based on BPDA formed a smectic C (SmC) phase as well as a SmA phase.

Introduction

Recent integration, miniaturization, and high functionalization in electronics are rapidly progressing, where both conductors and insulating materials have been packaged as densely as possible. The low thermal conductivity of insulating polymers yields a large temperature rise and gradient in devices that causes electric connection failure and reduces the lifetime of these devices. Therefore, thermoconductive polymers which can release generated heat effectively are required in semiconductors as electric insulators. To increase thermal conductivity, highly oriented polymers, that is, liquid crystalline (LC) polymers, are effective candidates.[1] The alignments of LC polymers are controlled in common ways, such as stretching, rubbing, the magnetic field, and self-alignment.[2−5]

Aromatic polyimides are promising materials for the applications to aerospace and electronic devices due to their excellent physical and chemical properties, that is, they have outstanding thermal and chemical stabilities, mechanical properties, electrical properties, and radiation resistance.[6,7] Next-generation polymeric insulators with high thermal conductivity required relatively low phase transition temperatures and low elastic resistance for easy processing. Thus, LC polyimides possessing flexible spacer units are good candidates. A few LC polyimides with sequences of methylene or ethylene oxide units in the main chains have been reported, such as thermotropic LC polyimides with methylene units (8−12) from a special tetracarboxylic dianhydride, 4,4″-terphenyltetracarboxylic dianhydride and aliphatic diamines,[8−10] and segmented LC polyimides prepared from 3,3′,4,4′-tetracarboxybiphenyl dianhydride (BPDA) and α,ω-bis(4-aminophenoxy)oxyethylene units.[11] These polyimides showed liquid crystallinity and lower phase transition temperatures compared to the polyimides based on BPDA and diamines with methylene spacer units (> 350 °C). For practical applications, a further decrease in fabrication temperatures is required to avoid oxidation of the copper wires inside integrated circuits (ICs). It is well-known that a siloxane unit is highly flexible, thus polyimides containing siloxane linkages are expected to show lower LC transition temperatures.

In a preceding work, we briefly reported the synthesis of LC polyimides with flexible siloxane spacer units (Scheme 1).[12] These polyimides exhibited high thermal stability and lower LC temperatures compared to the corresponding polyimides containing alkylene or ethylene spacer units.

In this report, we describe the extensive synthesis of novel LC polyimides derived from pyromellitic dianhydride (PMDA) or BPDA with diamines containing siloxane spacer units and their thermotropic LC behavior in detail. We have demonstrated two approaches for decreasing the crystal−LC transition temperatures of LC polyimides. One is the further extension of the length of the siloxane units and/or alkyl chains. The other involves twisting the imide planes of mesogenic units by the ortho-substituted methyl group, leading to a weakening of the intermolecular interaction of the imide planes. The relationship between molecular designs and LC behavior is discussed in detail.

Results and Discussion

Synthesis of Diamines and Polyimides. The diamine monomers containing siloxane linkages (**3a**−**3e**) were synthesized under the standard conditions for Williamson's ether synthesis, hydrosilylation, and reduction, as shown in Scheme 2. The reaction of 4-nitrophenol or 3-methyl-4-nitrophenol with 4-bromo-1-butene or 6-bromo-1-hexene yielded **1a**−**1c** in the presence of potassium carbonate in acetonitrile. The hydrosilylation of compound **1a**, **1b**, or **1c** with 1,1,3,3-tetramethyldisiloxane, 1,1,3,3,5,5-hexamethyltrisiloxane, or 1,1,3,3,5,5,7,7-octamethyltetrasiloxane in the presence of Karstedt's catalyst gave compound **2**. Analytically pure compounds were obtained in good yields (65−97%) after purification, which were hydrogenated to prepare monomer diamines **3**.

*Corresponding author. E-mail: mueda@polymer.titech.ac.jp.

Published on Web 12/04/2009

Figure 1 shows the ^1H and ^{13}C NMR spectra for diamine **3b** in $CDCl_3$. The signal positions in the ^1H NMR spectrum of **3b** are consistent with the proposed structures. The signals at 6.74 and 6.63 ppm can be assigned to the aromatic protons. Furthermore, the methyl protons adjacent to the silyl methyl groups appeared at 0.07 and 0.02 ppm. Similarly, the ^{13}C NMR spectrum shows the expected ten signals.

The LC polyimides **6** showing in Scheme 3 were prepared by using a two-step polycondensation procedure. PMDA (**4a**) or BPDA (**4b**) reacted with each diamine **3** at room temperature in *N*-methylpyrrolidone (NMP) to produce poly(amic acid)s (PAAs) **5** with high inherent viscosities in the range of 0.65−1.73 dL/g (Table 1). Then, polyimide films were obtained by thermal imidization of the PAAs cast on glass substrates under nitrogen, followed by immersion in warm water. In the representative FT-IR spectrum of prepared polyimide **6h**, the peaks for the amic acid groups disappeared and the characteristic imide peaks at 1770 (C═O asymmetric stretching), 1712 (C═O symmetric stretching), and 1389 cm^{-1} (C−N stretching) appeared, indicating complete imidization. In addition, strong absorption bands were also observed at 2958 and 1257 cm^{-1}, corresponding to C−H stretching of the alkyl groups and Si−C stretching of the siloxane groups, respectively, which further confirms the structures of the polyimides.

Thermal Properties. Analyses by TGA under nitrogen indicate that all polyimides **6** are thermally stable up to 400 °C (Table 1). The DSC curves of all polyimides **6b**−**6j** are shown in Figure 2. Except for polyimides **6d**, **6e**, and **6j**, all polyimides show more than two exothermic peaks upon cooling. Birefringence and fluidity were observed in the temperature range between these peaks by cross-polarizing microscopy. Therefore, the phase between the transition temperatures corresponds to a liquid crystalline phase. Compared with polyimides **6c** and **6h**, polyimide **6c** has higher crystalline−LC transition temperatures than polyimide **6h** because the aromatic and imide rings in the mesogenic units of polyimide **6c** are coplanar to one another, therefore the intermolecular interactions are stronger between each mesogenic unit than those of polyimide **6h**. As a result, polyimides **6a**−**c** and **6f**−**h** show lower crystalline-LC transition temperatures, 257 (**6b**), 214 (**6c**), 236 (**6f**), 236 (**6g**), and 203 °C (**6h**) on the second cooling by increasing the siloxane units because of the increasing flexibility of the main chains (Table 2, Figure 3). Moreover, we investigated polyimides **6d** and **6i** with longer methylene spacer units, which are expected to decrease the transition temperatures. However, there is no noticeable change in the temperatures observed by DSC, which suggests that the methylene units are less flexible than siloxane due to the gauche or trans conformational limitations and are therefore ineffective in decreasing the crystal-LC transition temperature. Interestingly, in the case of polyimides **6b**−**d**, the temperature range of LC behavior narrows as the spacer units become longer and, finally, polyimide **6d**, which has the longest spacer unit among **6b**−**d**, does not exhibit liquid crystallinity at all. On the other hand, polyimides **6e** and **6j**, with a methyl-substituted group in the mesogenic units, have also been designed to decrease transition temperatures. We expected that the twisted plane in the mesogenic units by the bulkiness of the methyl-substituted group weakened the intermolecular interaction, which led to a decrease in their transition temperatures. However, neither polyimide **6e** or **6j** show liquid crystallinity, but instead polyimides **6e** and **6j** exhibit a crystaline and an amorphous nature, respectively, by DSC trace and polarized optical microscopy (POM).

Scheme 1. Structure of Polyimides with Siloxane Spacers

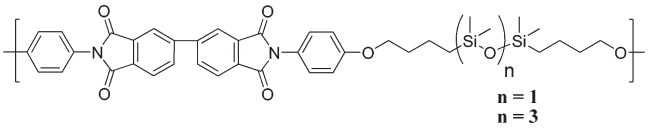

Scheme 2. Synthetic Routes of Monomers and Diamines 3

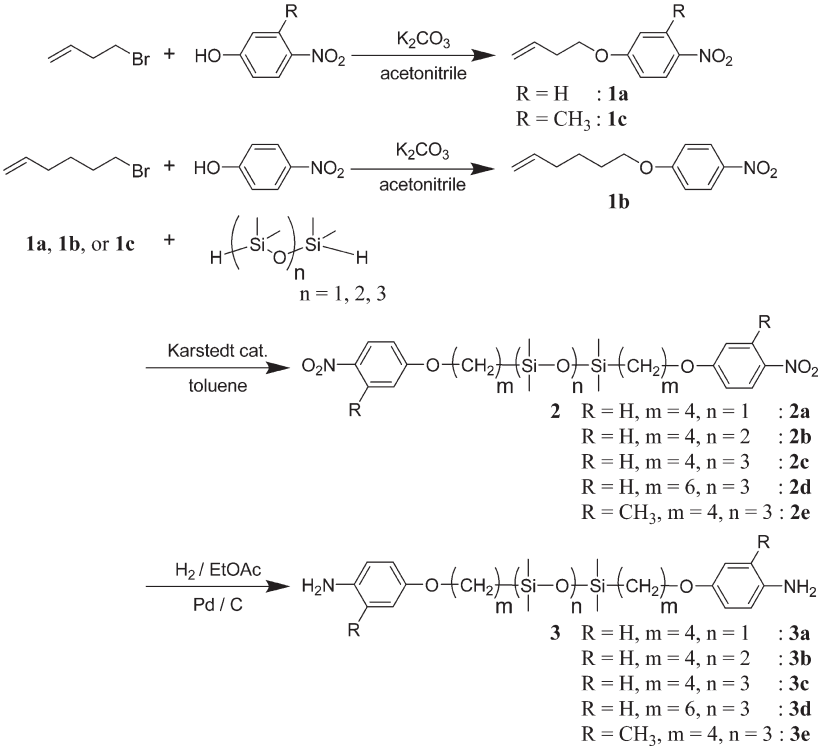

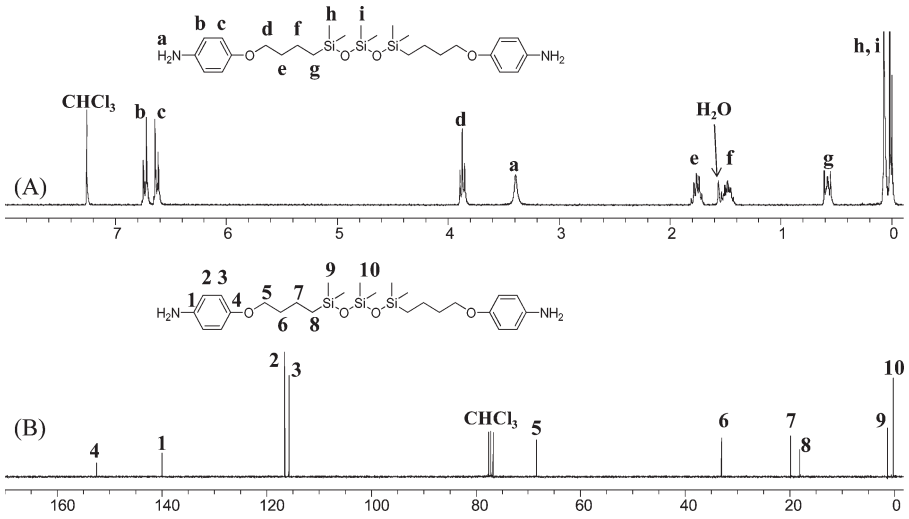

Figure 1. (A) ^{1}H and (B) ^{13}C NMR spectra of the diamine **3b**.

Scheme 3. Synthetic Routes of LC Polyimides 6

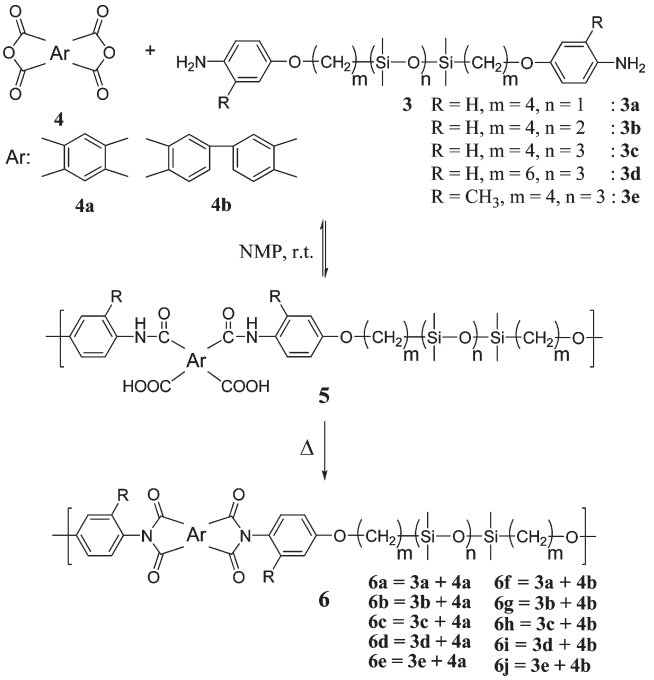

Thermotropic LC Behavior. Figure 4 shows the optical microscopic texture observed for the mesophase of polyimide **6h**. The clear fan-shaped texture observed here is assigned to smectic LC phase. A similar texture was observed in the mesophases of poyimides **6b**, **6c**, **6f**, **6h**, and **6i**. In order to identify the smectic structure, wide-angle X-ray diffraction (WAXD) measurements were performed for fibers spun from the isotropic melt. The typical X-ray patterns are shown in Figure 5, as observed for **6g**, which forms two LC phases. For the higher-temperature LC phase, sharp inner reflections are observed on the equator, i.e., along the fiber axis, and broad outer reflections are observed on the meridian (see Figure 5a). These profiles clearly show the formation of the SmA phase.[14] On cooling to a lower-temperature LC phase, the inner reflections are evidently split while the outer broad pattern is not significantly altered (Figure 5b), showing the transformation from the SmA to the SmC phase. The tilt angle of the molecules of the layer are elucidated as 22° from the splitting angle, which roughly

Table 1. Polymerization Results and Thermal Stabilities

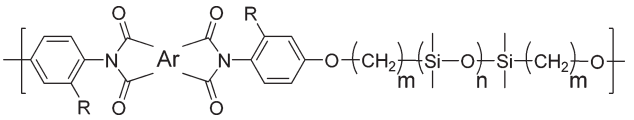

polymer	Ar	R	*m*	*n*	η_{inh} [dL/g][a]	$T_{d1\%}$ [°C][b]	$T_{d5\%}$ [°C][b]
6a	**4a**	H	4	1	0.72	399	454
6b	**4a**	H	4	2	0.73	426	456
6c	**4a**	H	4	3	0.66	415	455
6d	**4a**	H	6	3	0.79	428	454
6e	**4a**	CH_3	4	3	0.65	424	451
6f	**4b**	H	4	1	1.07	407	448
6g	**4b**	H	4	2	1.73	426	460
6h	**4b**	H	4	3	1.43	430	457
6i	**4b**	H	6	3	1.19	406	447
6j	**4b**	CH_3	4	3	0.78	408	452

[a] Inherent viscosities were measured at 30 °C in NMP at a PAA **5** concentration of 0.5 g/dL. [b] Decomposition temperature. $T_{d1\%}$: 1% weight loss temperature, $T_{d5\%}$: 5% weight loss temperature in the nitrogen atmosphere.

corresponds to 24° calculated from the layer spacing ratio of the SmA to the SmC phase. Polyimide **6h** also shows a similar SmA−SmC transformation, while **6b**, **6c**, **6f**, and **6j** form a single SmA phase before crystallization.

The present polyimides consist of three components, the aromatic, methylene and siloxane groups so the SmA structure can be illustrated as a microsegregation structure of three components (Figure 6). Referring to this structure, we compared the SmA layer spacings between homologous polyimides. Of interest is that the layer spacing of the SmA phase, i.e., the average length of the repeating unit, does not change significantly as the number of the siloxane units in the homologous series increases. For example, the layer spacings of SmA for **6f**, **6g**, and **6h** are 36.2, 36.1, and 35.9 Å, respectively, showing no expansion of layer spacing with an increase of two siloxane units (Table 2).[15] From a comparison of **6h** and **6i**, however, the SmA layer spacing increases from 35.9 to 39.1 Å; an increase of four methylene units causes a 3.2 Å increase in layer spacing. Thus, it can be concluded that the alkylene parts in the flexible spacer take a relatively extended shape, conforming similarly to the orientational order of the LC, as in the usual case of main-chain LC polymers,[14] while the siloxane parts are not extended at all. In other words, the cross sectional area of the siloxane

microdomain should be increased to a significant extent, which spontaneously leads to the unusually large cross sectional areas of the alkylene and mesogenic microdomains. In fact, this trend can be found to express on the spacing of the broad reflection that corresponds to the averaged lateral distance of polymers. In Figure 7, 2θ intensity profiles on the equator obtained in the SmA phases of **6f**, **6g**, **6h**, and **6i** are shown. From these intensity profiles, one can find that the peak position of the outer broad reflections gradually shifts from 5.5 to 6.4 Å with an increase in siloxane units. These values are considerably larger than the 4.8 Å observed in the analogous polyimide BPDA/6OE, consisting of a BPDA mesogen and polyoxyethylene spacer with 6 oxyethylene units.[16] Furthermore, of interest is that the outer broad reflection profile seems to have two maximum peaks in the SmA phases in **6b** and **6c**. The corresponding spacings are

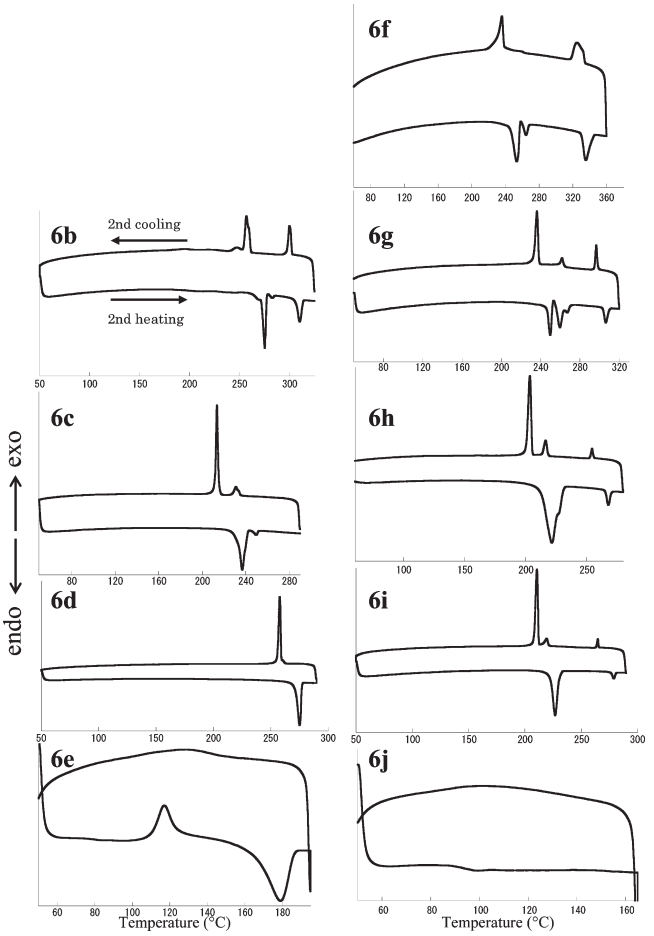

Figure 2. DSC heating and cooling curves of polyimides **6** by the measurement performed at a scanning rate of 10 °C/min.

Table 2. Thermal Transition Temperatures of Polyimides 6

polymer	Ar	R	*m*	*n*	$T_{cr\text{-}lc}$ [°C][a]	$T_{lc\text{-}lc}$ [°C][a]	$T_{lc\text{-}i}$ [°C][a]	d_{LC1} [Å]	d_{LC2} [Å]
6a	**4a**	H	1	4	b	b	b		
6b	**4a**	H	2	4	257	c	300		30.8
6c	**4a**	H	3	4	214	c	231		32.7
6d	**4a**	H	3	6	d	d	d		
6e	**4a**	CH_3	3	4	e	e	e		
6f	**4b**	H	1	4	236	c	325		36.2
6g	**4b**	H	2	4	236	262	297	34.7	36.1
6h	**4b**	H	3	4	203	216	254	32.6	35.9
6i	**4b**	H	3	6	211	219	265		39.1
6j	**4b**	CH_3	3	4	e	e	e		

[a] Peak-top temperatures determined by DSC at a second cooling rate of 10 °C/min. $T_{cr\text{-}lc}$: crystal−LC transition temperature, $T_{lc\text{-}lc}$: LC−LC transition temperature, $T_{lc\text{-}i}$: LC−isotropic transition temperature. [b] No data because of a too high transition temperature (> 330 °C) by POM. [c] No detection of LC−LC transition temperature. [d] There is no LC phase. $T_{cr\text{-}i}$ = 258 [°C] at a second cooling. [e] Crystalline polyimide **6e**. T_g = 79 [°C], T_c = 117 [°C], and T_m = 179 [°C] at a second heating. Amorphous polyimide **6j**. T_g = 91 [°C]. T_g: glass transition temperature, T_c: crystallization temperature, T_m: melting temperature.

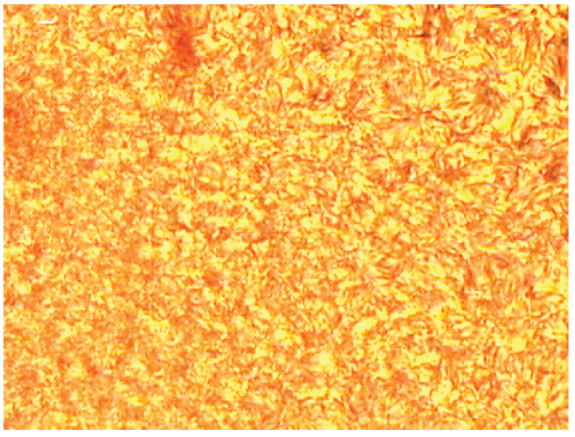

Figure 4. Polarized optical microscopic texture observed for SmA of polyimide **6h** at 245 °C.

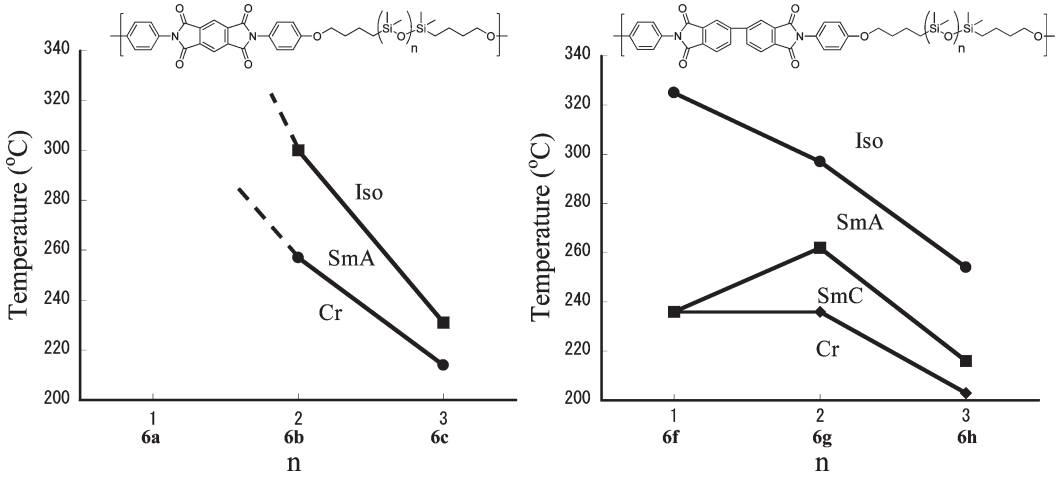

Figure 3. Plots of phase transition temperatures of polyimides **6** on the second cooling.

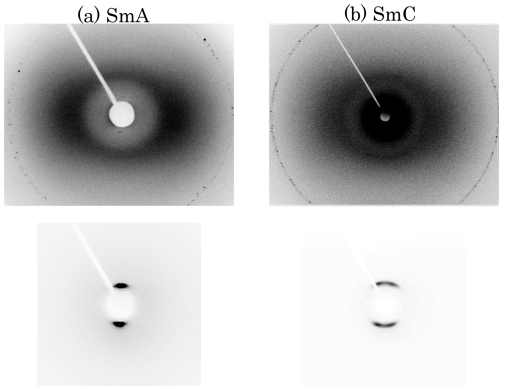

Figure 5. Wide angle X-ray diffraction patterns of (a) SmA and (b) SmC phases observed in the fiber samples of **6g**. To show the smectic layer reflection, the small angle region is enlarged in the lower photographs. Fiber axis is set in a vertical direction.

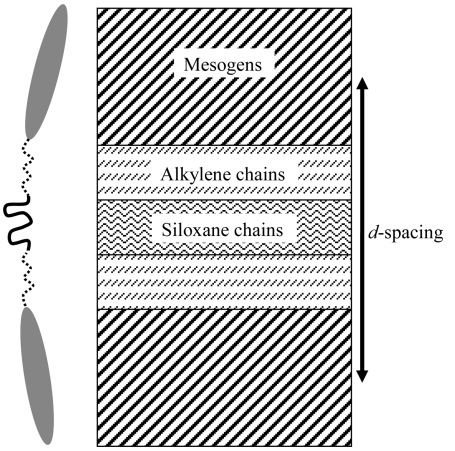

Figure 6. Schematic illustration of SmA layer structure in which aromatic, methylene, and siloxane groups are segregated to form sublayers.

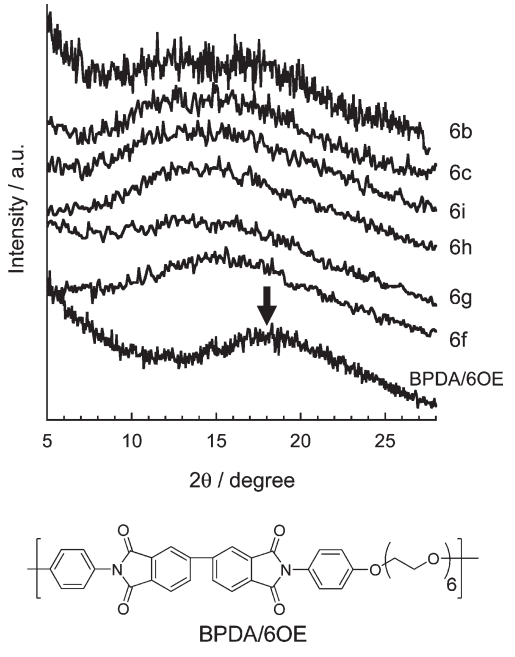

Figure 7. 2θ intensity profiles of outer broad reflections for fiber SmA samples of **6b**, **6c**, **6h**, **6i**, **6g**, and **6f**. As a reference, the profile observed for the SmA of BPDA/6OE without polysiloxane spacer (refer to the text) is shown. The arrow indicates the peak position of 4.5 $Å^{-1}$ normally observed in the LC phases of main-chain polymers.

7.3 and 5.3 Å for **6c**. Such an appearance of two outer broad reflections has been observed in similar main-chain polymers including the siloxane spacer,[15] and suggests the biaxiality of SmA.[17] Thus, the present polymers including the siloxane unit show some abnormality in their smectic structure formation, which will be analyzed in a future study.

In the course of this study, it was found that all transition temperatures of polyimides **6** became much lower simply by increasing the siloxane units. LC polymers with shorter flexible spacer units are desirable to achieve high thermal conductivity for IC applications. Therefore, the siloxane units indicated the superiority of the alkylene chains for decreasing the transition temperatures and the obtained polyimides are candidates as high thermal conductive polymers.

Conclusions

We have synthesized a new series of LC semialiphatic polyimides containing siloxane spacer units. They showed higher thermal stabilities ($T_{d5\%}$ > ~450 °C) and lower crystal−LC transition temperatures, 275 (**6b**), 237 (**6c**), 253 (**6f**), 250 (**6g**), and 222 °C (**6h**), compared to polyimides containing alkylene or oxyethylene spacer units. The transition temperature decreased by the increasing siloxane spacer units, as expected. On the other hand, the methyl-substituted polyimides aiming at twisting the coplanar imide rings and loosening the packing of the mesogens did not show liquid crystallinity, unfortunately. WAXD experiments confirmed the layered morphologies of LC polyimides with siloxane spacer units and their *d*-spacings. A smectic-A phase was formed in the polyimides derived from PMDA, while the polyimides based on BPDA formed a smectic-C phase as well as a smectic-A phase. Moreover, the layer spacings of SmA indicated that the alkylene chains in the flexible spacer take a relatively extended conformation, while the siloxane units are not extended at all. From 2θ intensity profiles, the peak position of the outer broad reflections gradually shifts from 5.5 to 6.4 Å with an increase of siloxane units. Further, there is the possibility that the biaxiality in the polyimides is derived from PMDA. A detailed investigation of this interesting abnormality is in progress. We also expect that these polyimides will exhibit relatively high thermal conductivity combining with a small amount of thermal conducting fillers and may possibly be used as insulators in electronics fields.

Experimental Section

Measurements. FT-IR spectra were measured on a Horiba FT-720 spectrometer. ^1H and ^{13}C NMR spectra were recorded with a Bruker DPX300S spectrometer. Inherent viscosities were measured at 30 °C in NMP at a polymer concentration of 0.5 g/dL. The transition characteristics were surveyed with a polarizing microscope (OLYMPUS BX51), together with the use of a LINKAM LTS-350 hot-stage equipped with a temperature controller by setting a polyimide film between crossed polarizers. Thermal analysis was performed on a Seiko EXSTAR 6000 TG/DTA 6300 thermal analyzer at a heating rate of 10 °C/min for thermogravimetry (TG) and a Perkin-Elmer DSC7 calorimeter connected to a cooling system at a heating rate of 10 °C/min for differential scanning calorimetry (DSC). WAXD measurements were performed at ambient temperature by using a Rigaku-Denki RINT-2500 X-ray generator with monochromic Cu Kα radiation (40 kV, 50 mA) from graphite crystal of monochromator and flat-plate type of imaging plate.

Materials. PMDA and BPDA were purified by sublimation prior to use. NMP, acetonitrile and toluene were purified by distillation. Other reagents and solvents were obtained commercially and used as received.

General Synthesis for Diamines. The diamine monomers containing siloxane linkages (**3a**−**3e**) were synthesized under the standard conditions for Williamson's ether synthesis, hydrosilylation, and reduction. As a typical experiment, the synthesis of diamine **3a** was described as follows. Detailed synthesis and characterization of other diamines (**3b**−**3e**) are described in Supporting Information.

Synthesis of 4-(3-Butenyloxy)nitrobenzene (***1a***). The title compound, **1a**, was synthesized according to the literature.[13] To a solution of 4-nitrophenol (0.423 g, 3.04 mmol) and K_2CO_3 (1.11 g, 8.02 mmol) in CH_3CN (20 mL) was added 4-bromo-1-butene (0.827 g, 6.13 mmol), and the mixture was refluxed for overnight. The solution was filtered through Celite and the filtrate was concentrated under reduced pressure. The residue was dissolved in CH_2Cl_2, washed with water, dried over $MgSO_4$, and the solvent was removed under reduced pressure to give a **1a** yellow residue, which was flash-chromatographed to give **1a** (yellow oil, 0.57 g, 97% yield). IR (NaCl), ν (cm^{-1}): 2942.8 (alkyl C−H), 1643.1 (C═C), 1592.9 (Ar C−C), 1508.1, 1334.5 (−NO_2). ^{1}H NMR (300 MHz, $CDCl_3$, δ, ppm, 25 °C): 8.20 (d, J = 9.3, ArH, 2H), 6.95 (d, J = 9.0, ArH, 2H), 5.96−5.82 (m, vinyl proton, 1H), 5.23−5.12 (m, vinyl proton, 2H), 4.11 (t, J = 6.6, −CH_2−, 2H), 2.62−2.55 (m, −CH_2−, 2H). ^{13}C NMR (75 MHz, $CDCl_3$, δ, ppm, 25 °C): 164.1, 141.5, 133.7, 125.9, 117.7, 114.5, 68.1, 33.4.

Synthesis of 1,3-Bis[4-(4-nitrophenoxy)butyl]-1,1,3,3-tetramethyldisiloxane (***2a***). To a solution of **1a** (0.519 g, 2.69 mmol) and 1,1,3,3-tetramethyldisiloxane (0.125 g, 0.934 mmol), in toluene (3 mL), Karstedt's catalyst (3 drops) (platinum divinyltetramethyldisiloxane complex in 2 wt % xylene) was added. The reaction mixture was refluxed under nitrogen for 24 h, then toluene was removed under reduced pressure. The residue was chromatographed (hexanes: CH_2Cl_2, 6:4) to give **2a**. The compound, **2a**, (0.321 g, 65% yield) was then isolated as a pale yellow oil after the vacuum. IR (NaCl), ν (cm^{-1}): 2950.6 (Alkyl C−H), 1592.9 (Ar C−C), 1515.8, 1338.4 (-NO_2), 1265.1 (Si−C). ^{1}H NMR (300 MHz, $CDCl_3$, δ, ppm, 25 °C): 8.19 (d, J = 9.0, ArH, 4H), 6.93 (d, J = 9.3, ArH, 4H), 4.04 (t, J = 6.3, −CH_2−, 4H), 1.88−1.79 (m, −CH_2−, 4H), 1.54−1.45 (m, −CH_2−, 4H), 0.61−0.55 (m, −CH_2−, 4H), 0.06 (s, Si-CH_3, 12H). ^{13}C NMR (75 MHz, $CDCl_3$, δ, ppm, 25 °C): 164.3, 141.4, 126.0, 114.5, 68.6, 32.5, 19.9, 18.1, 0.503. Anal. Calcd For $C_{24}H_{36}N_2$: C, 55.36 ; H, 6.97 ; N, 5.38. Found: C, 55.10 ; H, 6.91 ; N, 5.23.

Synthesis of 1,3-Bis[4-(4-aminophenoxy)butyl]-1,1,3,3-tetramethyldisiloxane (***3a***). A mixture of nitro compound **2a** (1.35 g, 2.60 mmol) and Pd/C (0.0393 g, 10 wt %) in EtOAc (10 mL) was stirred at room temperature for 2 days under hydrogen atmosphere by using a balloon. The solution was filtered through Celite and concentrated to give the diamine **3a** (1.18 g, 98% yield) as a light brown oil. IR (NaCl), ν (cm^{-1}): 3355.5 (N−H), 2950.6 (Alkyl C−H), 1623.8 (N−H), 1511.9 (Ar C−C), 1238.1 (Si−C). ^{1}H NMR (300 MHz, $CDCl_3$, δ, ppm, 25 °C): 6.74 (d, J = 9.0, ArH, 4H), 6.63 (d, J = 9.0, ArH, 4H), 3.87 (t, J = 6.3, −CH_2−, 4H), 3.40 (s, NH_2, 4H), 1.80−1.71 (m, −CH_2−, 4H), 1.54−1.42 (m, −CH_2−, 4H), 0.61−0.53 (m, −CH_2−, 4H), 0.05 (s, Si−CH_3, 12H). ^{13}C NMR (75 MHz, $CDCl_3$, δ, ppm, 25 °C): 152.5, 139.9, 116.5, 115.8, 68.4, 33.1, 20.0, 18.3, 0.510.

General Precedure for Polymer Synthesis. PMDA (**4a**) or BPDA (**4b**) was added to a solution of the diamines, **3**, in NMP, and the solution was stirred at room temperature for 12 h. Then a poly(amic acid) solution (15 wt %) was casted on a glass substrate and the imidization was carried out by heating in steps on hot-plate, finally the temperature was increased to 200 °C. Opaque yellow films, **6**, were obtained. Detailed synthesis and characterization of individual polyimides are described in Supporting Information.

Acknowledgment. The financial support from Mitsubishi Chemical Corporation is gratefully acknowledged.

Supporting Information Available: Text giving experimental details about the synthesis and characterization of **1b**−**1c**, **2b**−**2e**, **3b**−**3e**, and **6a**−**6j**. This material is available free of charge via the Internet at http://pubs.acs.org.

References and Notes

(1) Akatsuka, M.; Takezawa, Y. *J. Appl. Polym. Sci.* **2003**, *89*, 2464–2467.
(2) Osada, K.; Niwano, H.; Tokita, M.; Kawauchi, S.; Watanabe, J. *Macromolecules* **2000**, *33*, 7420–7425.
(3) Patil, H. P.; Lentz, D. M.; Hedden, R. C. *Macromolecules* **2009**, *42*, 3525–3531.
(4) Kato, T.; Nagahara, T.; Agari, Y.; Ochi, M. *J. Appl. Polym. Sci.* **2007**, *104*, 3453–3458.
(5) Harada, M.; Ochi, M.; Tobita, M.; Kimura, T.; Ishigaki, T.; Shimayama, N.; Aoki, H. *J. Polym. Sci., Part B: Polym. Phys.* **2003**, *41*, 1739–1743.
(6) Bessonov, M. I.; Koton, M. M.; Kudryavstev, V. V.; Laius, L. A. In *Polyimides: Thermally Stable Polymers*; Consultants Bureau: New York, 1987.
(7) Wilson, D.; Stenzenberger, H. D.; Hergenrother, P. *Polyimides*: Blackie: New York, 1990.
(8) Inoue, T.; Kakimoto, M.; Imai, Y.; Watanabe, J. *Macromol. Chem. Phys.* **1997**, *198*, 519–530.
(9) Kaneko, T. I.; Imamura, K.; Watanabe, J. *Macromolecules* **1997**, *30*, 4244–4246.
(10) Huang, H. W.; Kaneko, T. I.; Horie, K.; Watanabe, J. *Polymer* **1999**, *40*, 3821–3828.
(11) Coatat, G.; Eastmond, G. C.; Fairclough, J. P. A.; Paprotny, J.; Ryan, A. J.; Stagnaro, P. *Macromolecules* **2008**, *41*, 1034–1040.
(12) Shoji, Y.; Higashihara, T.; Watanabe, J.; Ueda, M. *Chem. Lett.* **2009**, *38*, 716–717.
(13) Lipshutz, B. H.; Ghorai, S.; Boskovic, Z. V. *Tetrahedron* **2008**, *64*, 6949–6954.
(14) Watanabe, J.; Hayashi, M. *Macromolecules* **1988**, *21*, 278.
(15) Braun, F.; Willner, L.; Hess, M.; Kosfeld, R. *Makromol. Chem.* **1990**, *191*, 1775.
(16) We synthesized LC polyimide with 6 oxyethylene units (BPDA/6OE) according to the previous report (n = 6) (see ref 11). Inherent viscosity was 1.04 dL/g. Transition temperatures of BPDA/6OE were determined to be $T_{cr\text{-}lc}$ = 239 °C and $T_{lc\text{-}i}$ = 282 °C on the second heating.
(17) Chandrasekhar, S.; Nair, G. G.; Rao, S. D.S.; Prasad, S.; Krishna, P. K.; Blunk, D. *Liq. Cryst.* **1998**, *24*, 67.